Separating topographical and chemical analysis of nanostructure of polymer composite in low voltage SEM

Separating topographical and chemical analysis of nano-structure of polymer composite in low voltage SEM

Q Wan[1], R A Plenderleith[1], M Dapor[3], S Rimmer[2], F Claeyssens[1], C Rodenburg[1]

[1]Department of Material Science and Engineering, University of Sheffield, Western Bank, Sheffield, S10 2TN, UK

[1]Department of Chemistry, University of Sheffield, Western Bank, Sheffield, S10 2TN, UK

[3]European Centre for Theoretical Studies in Nuclear Physics and Related Areas (ECT*-FBK) and Trento Institute for Fundamental Physics and Applications (TIFPA-INFN), via Sommarive 18, I-38123 Trento, Italy

Email: qwan2@sheffield.ac.uk

Abstract. The possibility of separating the topographical and chemical information in a polymer nano-composite using low-voltage SEM imaging is demonstrated, when images are acquired with a Concentric Backscattered (CBS) detector. This separation of chemical and topographical information is based on the different angular distribution of electron scattering which were calculated using a Monte Carlo simulation. The simulation based on angular restricted detection was applied to a semi-branched PNIPAM/PEGDA interpenetration network for which a linear relationship of topography SEM contrast and feature height data was observed.

1. Introduction

Due to the strong dependence of functional properties of polymer nano-composites on nano-morphological features, the characterization of nano-scale morphology is vital in the field of polymer nano-composite materials. Among all the techniques developed to provide morphological information, the SEM techniques processes several advantages: the simple sample preparation, contact free measurement, reasonable resolution in surface imaging and convenient scanning of a relatively large area comparing to other microscopies such as Transmission Electron Microscopy (TEM)[1] and Scanning Probe Microscopy (SPM)[2].

   Low-voltage (LV) SEM was developed in order to overcome the radiation damage on beam-sensitive samples, still avoiding the need of conductive coatings[3]. Earlier application of LVSEM to materials such as regenerated silk fiboin nanofibre[4] and bone grafting[5] has proved to be an efficient technique. However in the condition of low-voltage SEM the energy of the backscattered electrons (BSE) may drop to similar levels of the secondary electrons (SE), and the normal separate detection of the SE and BSE may not be applicable. Thus effort to achieve separated topography and chemical information from SEM image contrast were made by the introduction of the theories of electron scattering in the imaging process. As shown in the studies of natural fibre[6] and metal[7] samples this electron kinetic based detection provided a potential extraction of topography and chemical contrast. The recent study on the photovoltaic materials has pushed this detection technique further to predictable material contrast mapping and identification[8].

The distribution of the scattered electrons may be analyzed for SE or BSE in several aspects such as the kinetic energy, the impact depth and the scattering angle. Using a concentric backscattered detector which can potentially detected ~50 eV signal[9], we have chosen the scattering angle of the backscattered electrons as the main factor in our separation of topographical and chemical information.

2. Experimental

The 0%, 5%, 10%, 20% and 30% extracted PNIPAM branched PNIPAM/PEGDA interpenetration network sample (the synthesis process is described in reference[10]) was treated with a Diener Zepto version B plasma cleaner. The gas input was air, and etching condition was set to 840 s with a power of 100 W. The plasma chamber was ventilated once during the etching to avoid overheating the sample surface. The AFM height data were acquired with a Dimension 3100 AFM in tapping mode. The PNIPAM/PEG samples were imaged by a FEI NOVA 450 SEM in low-voltage conditions (<5 kV accelerating voltage) and the spot size was set to 2 in all images. SEM images were taken using a concentric backscattered detector with 4000 V beam deceleration field in working distance ~4 mm. The applied detector segment and the accelerating voltage are listed for individual images.

3.Result and Discussion

According to the definition of contrast, the simulated image BSE contrast, C_s, can be described by the equation 1, as follows:

$$C_s = \frac{I_s - I_s'}{I_s'}$$

(1)

where I_s is the simulated BSE signal of the sample PNIPAM, and I_s' is the simulated BSE signal of the background (PEGDA matrix).
The calculation of the simulated BSE signal, I_s, is based on the equation

$$I_s \propto \eta \sum_{\theta_1}^{\theta_2} P_{elastic}(\theta)$$

(2)

where $P_{elastic}$ is probability of electron elastic scattering at angle θ, θ_1 and θ_2 are respectively the minimum and the maximum of the range of scattering angles for a given detector segment, and η is the backscattering coefficient of the respective material.

η is calculated by a Monte Carlo code and $P_{elastic}$ is computed by using the Mott theory (details of the Monte Carlo method and of the Mott theory are described in reference[11]). The CBS detector was installed at the end of the objective lens pole piece. The angular range of each CBS detector segment was calculated by the measurement of inner segment size and by literature data[9]. The diameter of the inner segment A is 4 mm and each segment is 0.8 mm wide. The working distance as set on the microscope was kept close to 4mm.

For our imaging condition of 700 V primary beam we found to be η=0.135 for PNIPAM and η=0.118 for PEGDA. The angular probability on each detector segment is shown in figure 1(a).

The comparison of simulation (C_s) with the experiment (C_e) in figure 1(b) shows that the backscattered electron signal dominates in the inner segments, especially in segments B and C, which allows the chemical mapping with BSE using these segments.

The simulation also revealed that the BSE signal on the outer segment D on the CBS detector is very weak for materials using small working distances. C_s in segment D at 4 mm working distance would be ~ -1%. This means that PNIPAM is darker than PEGDA matrix. However the C_e in segment D is ~ 21%. Due to the very weak BSE contribution to the signal in segment D in the simulation, we expect that C_e in the segment D, stem mostly from SE and thus provides topography information for our chosen experimental settings. However we note that the electron distribution is sensitive to the

working condition of the microscope such as working distance and beam deceleration.
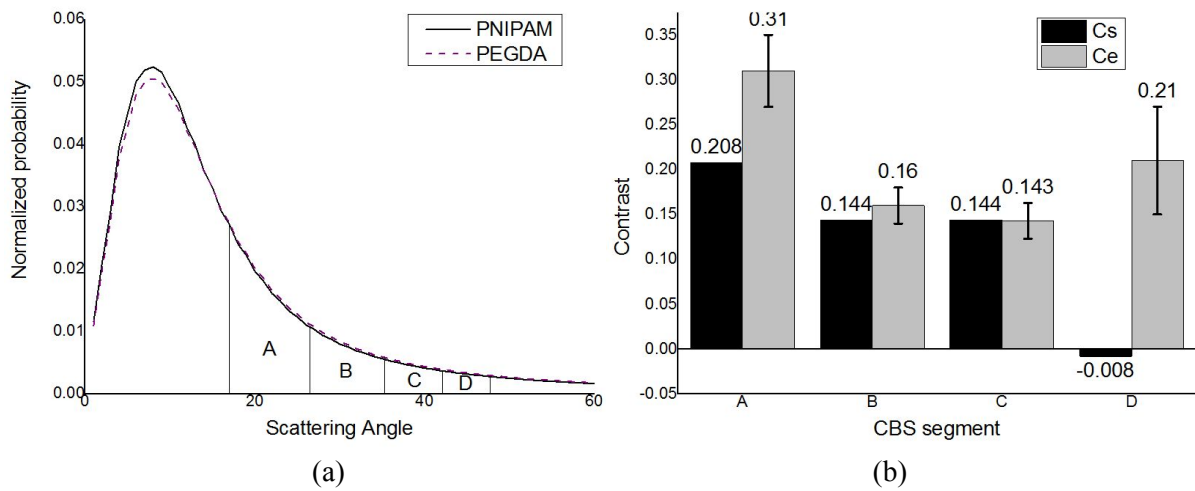

(a)   (b)

Figure 1: The angular probability of backscattering angle (a) and the C_s and C_e in segments A-D (b) for a 20% etched PNIPAM/PEGDA sample imaged with 700 V primary beam energy and 4mm working distance.

We have imaged the plasma etched and un-etched PNIPAM/PEGDA samples with segment D at primary energy 700 V and working distance 4 mm, and compared the contrast of topographic features including the PNIPAM particle and PEGDA matrix phase separation (Figure 2(a)) to AFM height data (Figure 3). We note that C_e of objects on the segment D images has a rather linear relationship with the respective height data measured by AFM. The PNIPAM particle data is almost proportional while the PEGDA phase separation deviates only slightly below 30 nm height (Figure 2(b)). We find that a linear relationship is valid in height range of 30-100 nm for our objects with <300 nm diameter.
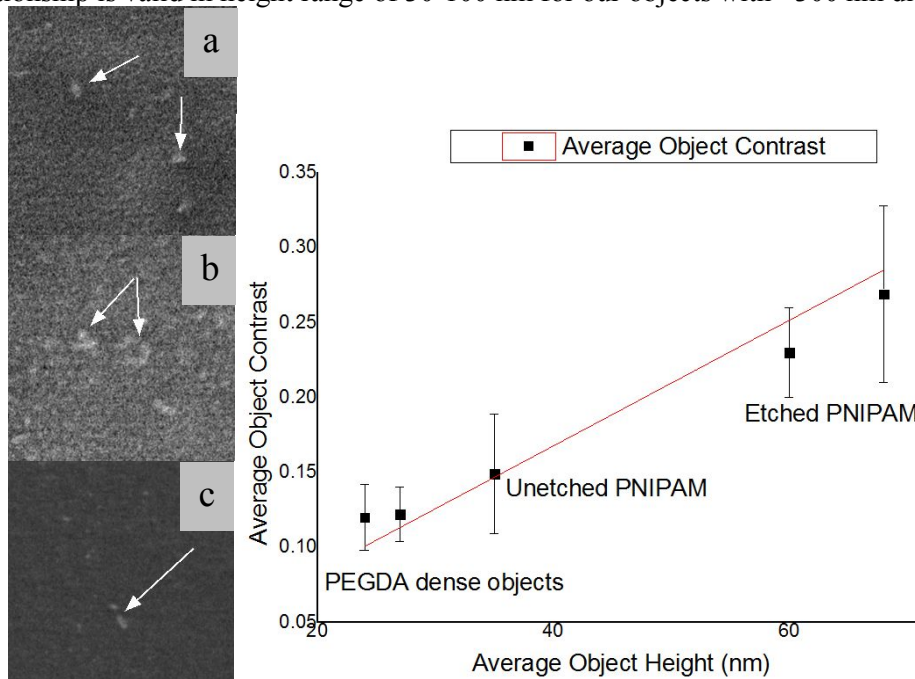

Figure 2: The CBS segment D image (normalized enhanced C_e) of 100 W/840 s plasma etched (a and b) and un-etched (c) PNIPAM particles and the average contrast vs average height of different objects..The field of view for SEM image is 2x2 µm. The PNIPAM particles are pointed out with arrows.
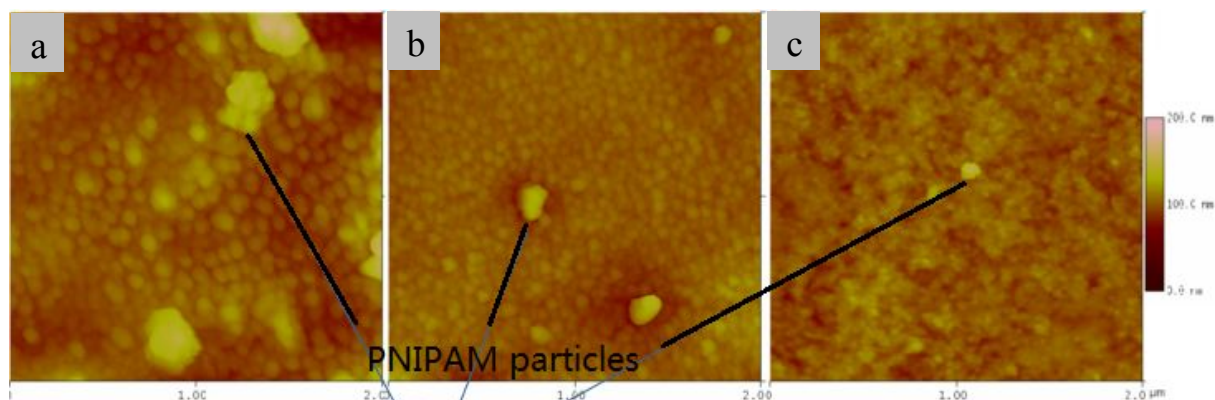
Figure 3: The AFM image of of 100 W/840 s plasma etched (a,b) and un-etched PNIPAM particles(c). The field of view in each image is 2x2 μm, the height range is 0-200 nm.

The deviation in the PEGDA phase separation feature may be due to the larger error in the measurement of smaller features by both AFM and SEM. More data on other materials should be collected to test the wider applicability for the linear height-contrast relationship. We note the peak in elastic scattering angular probability curve will shift to the smaller angles as the material becomes denser. Materials denser than our sample tend to have lower BSE signal in outer segment D. This indicates that our height mapping may still be reasonable for materials denser than our polymers.

4. Conclusion

The distribution of backscattered electrons was simulated and the separation of chemical and topographical information in LVSEM was achieved through the controlling of angular range of detection in our experiment. We found an approximately linear relationship between contrast C_e in CBS D segment and the AFM height data for two polymers. Such a relationship therefore could be used for contact free direct height mapping of nano-topographical features in LV-SEM once a calibration curve is recorded. Simulations suggest the wider applicability to denser materials.

References

[1] Danino D, 2012 *Curr Opin Colloid Interface Sci*, **17** 316
[2] Vansteenkiste S O, Davies M C, Roberts C J, Tendler S J B, Williams P M, 1998 *Prog Surf Sci*, **57** 95
[3] Vezie D L, Thomas E L, Adams W W, 1995 *Polymer*, **36** 1761
[4] Mhuka V, Dube S, Nindi M M, Torto N, 2013 *Macromol Res*, **21** 995
[5] Benezra Rosen V, Hobbs L W, Spector M, 2002 *Biomaterials*, **23** 921
[6] Rasch R, Stricher A, Truss R W, 2013 *J. Appl Polym Sci*, **131**
[7] Nagoshi M, Aoyama T, Sato K, 2013 *Ultramicroscopy*, **124** 20
[8] Masters R C et al, 2015 *Nat Commun*, **6** 6928
[9] Sakic A et al, 2011 *Micro Technology and Micro Devices SAFE, 1-4*
[10] Plenderleith R, 2014 *thesis* University of Sheffield
[11] Dapor M, 2014 *Transport of Energetic Electrons in Solids*, Springer. Tr. Mod. Phys., Vol. 257 (Springer, Berlin)